Journal of Colloid and Interface Science 395 (2013) 40–44

Contents lists available at SciVerse ScienceDirect

Journal of Colloid and Interface Science

www.elsevier.com/locate/jcis

Microstructures, surface states and field emission mechanism of graphene–tin/tin oxide hybrids

Jijun Ding [a,b], Minqiang Wang [a,b,*], Xingbin Yan [c], Xiangyu Zhang [a,b], Chenxin Ran [a,b], Haixia Chen [d] Xi Yao [a,b]

[a] Electronic Materials Research Laboratory, Key Laboratory of Ministry of Education, School of Electronic and Information Engineering, Xi'an Jiaotong University, Xi'an 710049, China
[b] International Center for Dielectric Research, Xi'an Jiaotong University, Xi'an 710049, China
[c] State Key Laboratory of Solid Lubrication, Lanzhou Institute of Chemical Physics, Chinese Academy of Sciences, Lanzhou 730000, China
[d] School of Science, Xi'an Shiyou University, Xi'an 710065, China

ARTICLE INFO

Article history:
Received 6 October 2012
Accepted 5 November 2012
Available online 15 November 2012

Keywords:
Graphene–Sn/SnO_2 hybrids
Microstructures
Surface state
Field emission mechanism

ABSTRACT

The effects of microstructures and surface states on the field emission, which are important to a good understanding of the field emission mechanism, are unclear. In this paper, the microstructures and surface states of graphene–Sn/SnO_2 hybrids were analyzed, and the field emission mechanism was explored. Raman spectra and images revealed that SnO_2/Sn droplets are strongly bound on graphene surface, and there exist oxygen vacancies at the surface of graphene–Sn/SnO_2 hybrids. Among X-ray photoelectron spectroscopy spectra, the peak of O 1s shifts 1.6 eV toward higher binding energies in the 5 min sample with the best field emission properties, which indicates that the field emission improvement in graphene–Sn/SnO_2 hybrids arises from the band-bending effect and a lower work function.

1. Introduction

Graphene as a two-dimensional macromolecular sheet of carbon atoms has superior electrical conductivity and mechanical properties [1,2], which would make it an excellent electron transport material, even more appropriate than C_{60}, polyaniline, graphite-like carbon [3]. Zhang et al. [4] reported that graphene has a high level of emission current at a low external electric field. Li et al. [5] reported temperature dependence of the field emission from the few-layer graphene films. Stratakis et al. [6] found that field emission properties of microstructured silicon vertices can be enhanced by depositing free-standing graphene. These results suggest that graphene might also be an attractive material for electron transport in field emission displays.

Field emission properties of SnO_2 have been explored extensively [7–9]. Researchers have also attempted to further improve the field emission properties of SnO_2. Such as, Wang et al. [10] reported that highly oriented SnO_2 nanorod arrays have more excellent field emission than SnO_2 films. Wu [11] fabricated Sb doped SnO_2 nanowires, he found that the field emission of SnO_2 nanowires was improved by doping Sb. Jang et al. [12] concluded that posttreatment of H_2 exposure can be an available process for improving the field emission properties of either SnO_2 nanowire or nanorod.

Graphene–SnO_2 hybrids have also been prepared by various methods [13–15]. Such as, Lian et al. [16] prepared graphene–SnO_2 hybrids by a gas–liquid interfacial synthesis approach. Zhang et al. [17] synthesized SnO_2 nanorods on graphene by a straightforward nanocrystal-seeds-directing hydrothermal method. Wang et al. [18] prepared graphene–SnO_2 hybrids involving solution-based chemical synthesis, spray drying, and annealing. Graphene–SnO_2 hybrids can also be formed by in situ reduction/oxidation [19]. Our previous work [20] has also shown that few-layer graphene and SnO_2 (G–Sn/SnO_2) hybrids are good electron emitters. However, the field emission mechanisms of G–Sn/SnO_2 hybrids are still controversial. Furthermore, the effects of microstructures and surface states on the field emission of hybrids, which are important to a good understanding of the electron emission mechanism, are unclear. In this paper, G–Sn/SnO_2 hybrids were prepared on n-Si(100) substrates. The crystal structures, microstructures, optical properties, surface states of G–Sn/SnO_2 hybrids were analyzed by using X-ray diffraction (XRD) pattern, transmission electron microscopy (TEM) images, laser Raman spectra, X-ray photoelectron spectroscopy (XPS) spectra. The electron transport mechanism during field emission in G–Sn/SnO_2 hybrids is formulated based on the experimental results.

* Corresponding author at: Electronic Materials Research Laboratory, Key Laboratory of Ministry of Education, School of Electronic and Information Engineering, Xi'an Jiaotong University, Xi'an 710049, China. Fax: +86 29 82668794.
E-mail address: mqwang@mail.xjtu.edu.cn (M. Wang).

0021-9797/$ - see front matter
http://dx.doi.org/10.1016/j.jcis.2012.11.006

2. Experimental

Schematic illustration of fabricating process of the G–Sn/SnO_2 hybrids is shown in Fig. 1. The detail methods are given in our previous report [20]. XRD patterns were obtained on a Rigaku D/max-2400 X-ray diffractometer with Cu Ka radiation (λ = 0.15406 nm). TEM images were characterized by a JEOL JEM-2100 transmission electron microscope operated at 300 kV. Laser Raman spectra were investigated using a JY LabRAM HR800 laser Raman spectrometer from 100 to 3000 cm^{-1} at room temperature. The 514.5 nm line of the laser was used as the excitation source. XPS spectra were analyzed by a VG Scientific Corp MK-II X-ray photoelectron spectroscope.

3. Results and discussion

3.1. Microstructures of G–Sn/SnO_2 hybrids

Our previous work [20] reported that there are some small and compact droplets in scanning electron microscopy (SEM) image of SnO_2 films, while sphere flowers are formed after depositing graphene layer. In order to further investigate the microstructures of G–Sn/SnO_2 hybrids, it is necessary to obtain its TEM images. Fig. 2a shows TEM images of G–Sn/SnO_2 hybrids. One can see that transparent graphene is present over a large area, and the surfaces of the graphene are not perfectly flat, with wrinkles over the surface giving different levels of transparency. On the other hand, SnO_2 and/or Sn spherical droplets were attached to the surfaces of the graphene dispersedly. It should be noted that no droplets were found scattered outside graphene, even after sonication, which indicates that SnO_2 and/or Sn are strongly bound on graphene surface. This also confirms that G–Sn/SnO_2 hybrids could be successfully prepared.

Fig. 2b shows partial high-resolution TEM (HRTEM) image. The upper right inset shows distinct interplanar *d*-spacing of graphene, Sn and SnO_2, while the lower left inset shows more general HRTEM images of G–Sn/SnO_2 hybrids. The measured *d*-spacing is 0.337 nm in accordance with graphene (002) plane. The spherical droplets region show different interplanar *d*-spacing corresponding to the Sn and SnO_2 lattice plane, which was marked in the HRTEM images.

Fig. 3 shows Raman spectra of graphene, SnO_2 films, and G–Sn/SnO_2 hybrids. In the graphene spectrum, three sharp peaks at 1350, 1583, and 2695 cm^{-1} correspond to the D, G, and 2D peaks, respectively. Elias et al. [21] reported that the main features in the Raman spectra of carbon based materials are the D and G peaks that lie at around 1350 and 1580 cm^{-1}, respectively. The G peak corresponds to optical E_{2g} phonons at the Brillouin zone center, whereas the D peak is caused by breathing-like modes. The ratio of the intensity of the G-band to the D-band is related to the in-plane crystallite size [22]. Besides, the intensity ratio of I_G/I_D is widely used for characterizing the defect quantity in graphene, and a small ratio (I_G/I_D = 2.26 in this work [23]) indicates a large disorder arising from structural defects [24]. The ratio of I_G/I_{2D} can be used to determine the layers number of graphene, and the small ratio (I_G/I_{2D} = 0.71 in this work) shows the few number of layers. In addition, the full width at half-maximum (FWHM) of the 2D band is around 47.1 cm^{-1}, which lies within the range of 35–50 cm^{-1} observed for few-layered graphene systems [25]. For both SnO_2 films and G–Sn/SnO_2 hybrids, two strong peaks at 109.7 and 201.2 cm^{-1} and a wide band at 290–720 cm^{-1} were observed in the Raman spectra. Liu et al. reported a weak peak at 113.2 cm^{-1} and assigned it to SnO_2 B_{1g} mode [26]. In addition, Diéguez et al. [27] concluded that B_{1g} mode appears quite often with smaller nanoparticles but is difficult to locate due to its very low intensity with respect to the other modes. Mcguire et al. [28] confirmed that the peaks at 112 and 210 cm^{-1} were stoichiometric composition as SnO, and the peak at 171 cm^{-1} could be Sn_2O_3/Sn_3O_4 or some other unknown phase. However, in this study, two sharp peaks at 109.7 and 201.2 cm^{-1} with small FWHM were detected. So, the peak at 109.7 cm^{-1} can be assigned to the SnO peak. A new Raman peak appeared at 201.2 cm^{-1} was assigned to other tin oxides. In addition, a wide band at 290–720 cm^{-1} containing classical E_g and A_{1g} modes was observed in both SnO_2 films and G–Sn/SnO_2 hybrids because of structural distortions induced by disorders such as local lattice disorder, oxygen deficiencies arising from Sn at the interface and surface [26]. In our G–Sn/SnO_2 hybrids, its XPS indicated that

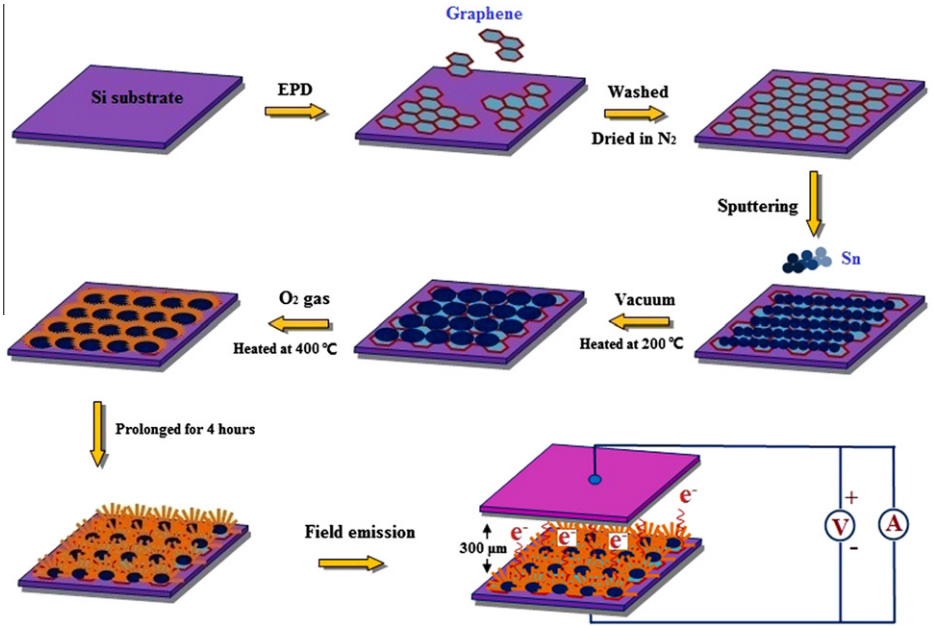

Fig. 1. Schematic illustration of fabricating process of the G–Sn/SnO_2 hybrids: (i–iii) graphene was deposited on Si substrate, (iv) Sn nanoparticles were sputtered on graphene-coated Si substrate, (v) formation of aggregated Sn droplets at 200 °C for 1 h, (vi) formation of SnO_2 nuclei on the surface of Sn droplets at 400 °C, (vii) prolonged for 4 h to form G–Sn/SnO_2 hybrids, and (viii) field emission measurement.